

Ultrasensitive Detection of DNA by PNA and Nanoparticle-Enhanced Surface Plasmon Resonance Imaging

Roberta D'Agata,^[a] Roberto Corradini,^[b] Giuseppe Grasso,^[a] Rosangela Marchelli,^[b] and Giuseppe Spoto^{*[a, c]}

Recently, DNA sensing by advanced technologies^[1] has become an important issue in various fields of life sciences for both applicative and research purposes.^[2,3] The real-time PCR (polymerase chain reaction) is the method of choice for quantitative analysis, although end-point PCR amplification followed by fluorescence detection of labeled DNA is extensively used. Massive miniaturized parallel analysis using DNA microarray technology can be envisaged,^[4] with DNA probes immobilized on surfaces. Since PCR involves time-consuming thermal cycles and is subject to severe contamination problems, however, a major challenge for rapid and reliable DNA analysis appears to be the development of rapid and multiplexed methods that 1) do not rely on PCR, and 2) are based on label-free detection systems.

SPR imaging (SPRI)^[5] has recently emerged as an extremely versatile method for detecting interactions of biomolecules in a microarray format.^[6–8] It uses optical detectors for spatial monitoring of localized differences in the reflectivity of the incident light ($\Delta\%R$)—which can be seen as brighter or darker regions in the SPR image—from an array of biomolecules linked to chemically modified gold surfaces. Label-free and real-time analyses can be carried out with high throughput and low sample consumption by coupling microfluidic devices with the SPRI apparatus.^[9,10]

However, the use of SPRI for genomic assays is limited by reduced sensitivity in the detection of hybridized DNA or RNA samples, so a number of different strategies directed towards amplifying SPRI response to DNA and RNA hybridization have recently been investigated,^[11,12] in particular with use of colloidal gold nanoparticles (AuNPs).^[13–15] On the other hand, another issue that deserves attention is the sequence specificity, in particular when single-nucleotide polymorphisms (SNPs) or point mutations are concerned.^[16–18]

Peptide nucleic acids^[19] (PNAs) have been shown to be able to improve both selectivity and sensitivity in targeting complementary DNA and RNA sequences.^[20,21] PNAs are DNA mimics in which the negatively phosphate deoxyribose backbone is replaced by a neutral *N*-(2-aminoethyl)glycine linkage. On ac-

count of their outstanding properties, PNAs have been proposed as valuable alternatives to oligonucleotide probes.^[3,22–25]

Surface plasmon optical detection of PNA:DNA and PNA:RNA hybridization has already been demonstrated,^[26,27] and the lack of sensitivity for unamplified DNA or RNA detection has been overcome either by coupling of spectral SPR with electrochemically based techniques (detection limit 10 pm)^[28] or by use of a fluorescence-based SPR technique known as surface plasmon fluorescence spectroscopy (detection limit 200 pm).^[23,25]

Here we report on the possibility of using PNA probes for the ultrasensitive nanoparticle-enhanced SPRI detection of DNA sequences down to 1 fm, while maintaining a very high selectivity in the recognition of single-nucleotide mismatches, through the use of microchannel devices. The experiments were carried out with a 15-mer PNA sequence (PNA 1, Figure 2, below) specifically designed to identify Roundup Ready (RR) genetically modified soybean, which had been tested by PNA microarray technology previously.^[3]

Figure 1 shows a representative SPR difference image obtained after the spatially controlled immobilization of PNA 1

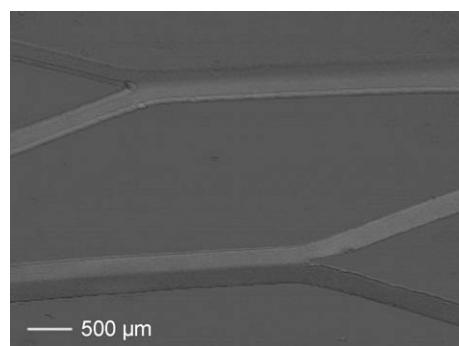


Figure 1. SPR difference image showing immobilization of PNA 1 probe (0.1 μ m in PBS). A Y-shaped microfluidic network was used for the experiment. The brighter areas identify the regions where the PNA immobilization occurred.

on a gold surface previously functionalized with dithiobis(*N*-succinimidylpropionate) (DTPS). Brighter regions within the Y-shaped microchannels define the areas where PNA 1 is immobilized (PNA 1 solution 0.1 μ m in PBS; surface coverage of 3×10^{12} molecules cm^{-2}), whereas darker regions in the microchannel areas were obtained by mPEG-NH₂ immobilization.

The DNA sequences used (36 mers) each contained a variable tract at the 3' terminal part—variously constituting the full match (DNA-FM) 15-mer target sequence, a singly mutated specimen (DNA-MIS-A,T,C), or an unrelated control sequence

[a] Dr. R. D'Agata, Dr. G. Grasso, Prof. G. Spoto

Dipartimento di Scienze Chimiche, Università di Catania
Viale Andrea Doria 6, 95125, Catania (Italy)

Fax: (+39) 095-580138
E-mail: gspoto@unict.it

[b] Prof. R. Corradini, Prof. R. Marchelli

Dipartimento di Chimica Organica ed Industriale, Università di Parma
V.le G. P. Usberti 17/a, 43100, Parma (Italy)

[c] Prof. G. Spoto

Istituto Biostrutture e Bioimmagini, CNR
Viale A. Doria 6, Catania (Italy)

Supporting information for this article is available on the WWW under <http://www.chembiochem.org> or from the author.

PNA-Target PNA 1	5'-AAACCCCTTAATCCCA-3'	AuNP-Target sequence DNA-12mer 5'-GCAGCTTATCGT-3'C6-Biotin
		T₉ spacer
Full-match sequence DNA-FM	3'-TTTGGGAATTAGGGT---TTTTTTTT---CGTCGAATAGCA-5'	
Mismatch sequences <i>X</i> =A,T,C DNA-MIS-X	3'-TTTGGXAATTAGGGT---TTTTTTTT---CGTCGAATAGCA-5'	
Control sequence DNA-CTR	3'-CGCATTGTGCCTCAC---TTTTTTTT---CGTCGAATAGCA-5'	
No spacer sequence DNA-NS	3'-TTTGGGAATTAGGGT-----CGTCGAATAGCA-5'	
Spacer primer sequence DNA-SP	3'-TTTGGGAATTAGGGT---TAAGGTTAA---CGTCGAATAGCA-5'	
	Variable region	Common region

Figure 2. Sequences and acronyms for the oligonucleotides used in this work.

(DNA-CTR)—followed by a T₉ spacer and then by an opportunely designed oligonucleotide 5'-tail (as target for the nanoparticle-linked DNA) (see Figure 2). The SPRI response after the direct hybridization of the 15-mer part of the DNA-FM target (1 μ M in PBS) complementary to the immobilized PNA 1 is shown in Figure 3A, where the change in percent reflectivity ($\Delta\%R$) over time caused by the target adsorption is reported.

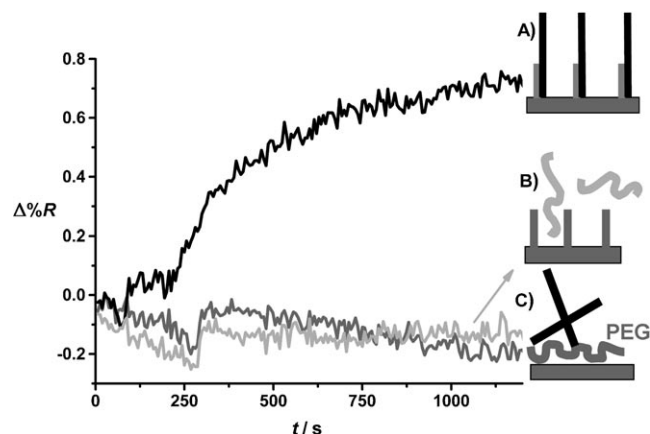
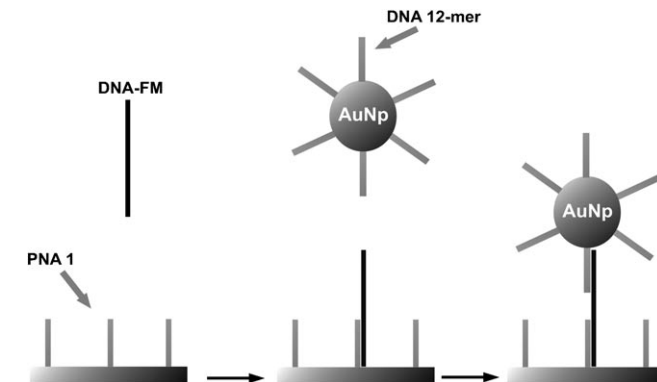


Figure 3. Change in percent reflectivity ($\Delta\%R$) over time obtained for the interaction between the surface-immobilized PNA 1 probe and A) DNA-FM (1 μ M) target, B) DNA-CTR (1 μ M) control sequence. C) The change in percent reflectivity over time obtained when the DNA-FM (1 μ M) was put in contact with a mPEG-modified surface is also shown.

The direct target hybridization at a 1 μ M concentration resulted in a $\Delta\%R$ value that was low ($\approx 0.7\%$), but higher than that obtained with the control sequence (DNA-CTR; Figure 3B), which was comparable to that obtained when the target (DNA-FM) was put in contact with a mPEG-modified surface (Figure 3C). This direct detection scheme, however, failed to detect target DNA at sub-micromolar concentrations.

AuNPs were used to achieve ultrasensitive detection of the target hybridization by following the sandwich strategy described in Scheme 1. A DNA-FM solution (concentration rang-

ing from 1 μ M to 1 fM, 150 μ L, flow rate 5 μ L min⁻¹) was injected into the microchannel containing the immobilized complementary PNA 1. AuNPs conjugated to a 12-mer oligonucleotide complementary to the final tract of the target DNA, not involved in the hybridization with the PNA 1 probe, were used to produce a detectable signal. The specificity of the DNA-FM adsorption was checked by comparing the nanoparticle-enhanced SPRI response with those obtained



Scheme 1. Pictorial description of the strategy used for the ultrasensitive nanoparticle-enhanced SPRI detection of the target DNA sequence.

when singly mismatched sequences (DNA-MIS-A, T, C) or the unrelated sequence (DNA-CTR) were allowed to interact with the surface-immobilized PNA 1. Figure 4 shows the SPRI responses obtained when 1 fM of target DNA-FM or mismatched or unrelated DNA solutions (1 fM) were used for the experiments. The $\Delta\%R$ caused by the nanoparticle-enhanced SPRI detection of the DNA-FM hybridization (average SPRI response $\Delta\%R=2.14$, SD=0.2, replicate measurements $n=5$) is different (t-test, $P=0.99$) from those generated after the adsorption of the single mismatch carrying sequences (DNA-MIS-T, DNA-MIS-A, DNA-MIS-C; average $\Delta\%R$, SD=0.29 \pm 0.04, $n=5$), as well as from those obtained with a DNA-CTR solution (1 fM), a DNA-FM solution (1 fM) adsorbed on an mPEG surface, and with no DNA adsorbed on the PNA 1 probe. Such results are visualized in Figure 4, which shows a representative SPR difference image of the parallel detection of the 1 fM sequence adsorption to PNA 1 and mPEG surfaces.

In order to demonstrate that similar results are also obtained in the absence of the T₉-spacer, experiments were also carried out with a target with no spacer (DNA-NS; see Figure 2) or with a different spacer (DNA-SP). The results obtained for 50 fM solutions are shown in Figure 5.

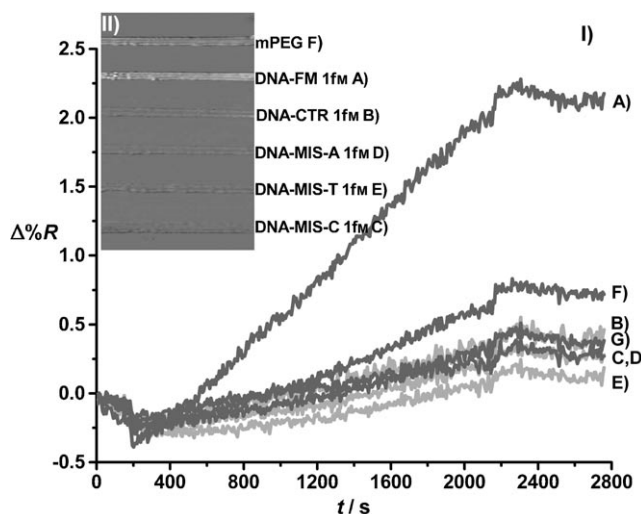


Figure 4. I) Time-dependent SPRI curves obtained after the adsorption of DNA 12-mer-AuNPs on: A) DNA-FM (1 fm) hybridized to the surface-immobilized PNA 1 probe, B) DNA-CTR (1 fm), C) DNA-MIS-C (1 fm), D) DNA-MIS-A (1 fm), and E) DNA-MIS-T (1 fm) adsorbed on surface immobilized PNA 1. F) DNA-FM (1 fm) adsorbed on a mPEG-modified gold surface, and G) PNA 1 probe surface with no DNA. The latter curve was obtained from a separate experiment. II) Representative SPR difference image showing the parallel detection of the SPRI responses described above.

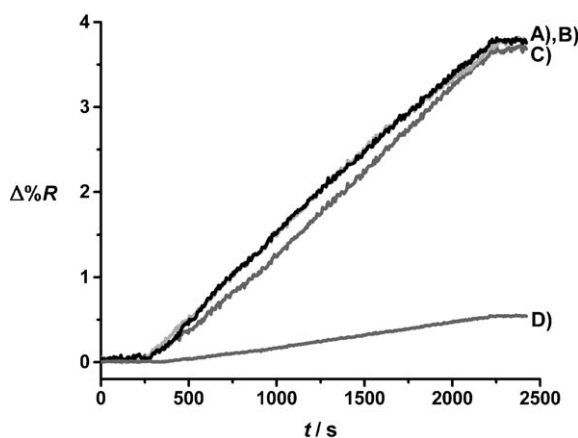


Figure 5. Time-dependent SPRI curves showing the nanoparticle-enhanced SPRI detection of A) DNA-SP, B) DNA-FM, and C) DNA-NS hybridization to the PNA 1. D) The nanoparticle-enhanced SPRI response obtained in the absence of DNA is also shown. The concentrations of the target solutions used for this experiment were 50 fm.

The experiments described demonstrate that the combination of the ultrasensitive nanoparticle-based SPRI biosensing with the high affinity and selectivity of the PNA allows the detection of DNA at a 1 fm concentration with use of only 150 zeptomoles of the target molecules and still presenting single-nucleotide mismatch recognition. This limit of detection is far below that previously obtained by us by microarray technology with the same PNA probe (1 nm, 50 fmol), for detecting RR-soy.^[3]

To the best of our knowledge, this is the first example of ultrasensitive SPRI detection of hybridization between PNA

probes and DNA targets. In fact, a 200 pm limit was recently reported for detection of PNA hybridization of single-stranded DNA by surface plasmon enhanced fluorescence spectroscopy,^[23] whereas a 10 fm sensitivity for the detection of single-stranded DNA by an oligonucleotide probe by use of a surface plasmon biosensor based on nanoparticle-enhanced diffraction gratings has been demonstrated.^[29] Discrimination of a completely different sequence (16 bases) was reported in the latter work as a test for specificity, whereas the method here reported mismatches involving single bases.

The responses ($\Delta\%R$) caused by the nanoparticle-enhanced SPRI detection (Scheme 1) of A) match and B) mismatch sequences as a function of concentration are reported in Figure 6. Maxima of the SPRI $\Delta\%R$ values were obtained at 1 nm

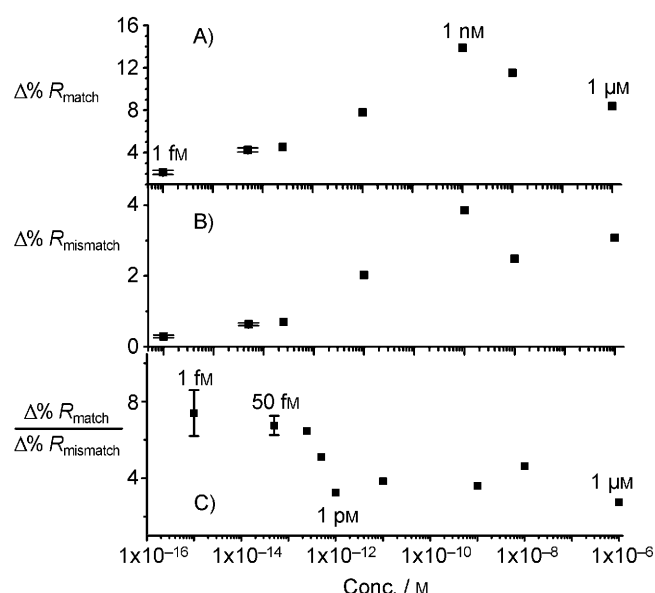


Figure 6. $\Delta\%R$ values obtained after nanoparticle-enhanced SPRI detection (see Scheme 1) of differently concentrated A) match and B) mismatch sequence solutions. The $\Delta\%R_{\text{mismatch}}$ values are the products of averaging of the DNA-MIS-C, DNA-MIS-A, and DNA-MIS-T SPRI responses. C) The ratios between $\Delta\%R_{\text{match}}$ and $\Delta\%R_{\text{mismatch}}$ as a function of logarithmic concentrations of the sequences used are also shown. The error bars show the standard deviations of the mean responses ($n=5$).

concentrations both of the match (Figure 6 A) and of the mismatch (Figure 6 B) sequences, although the latter show a much lower response, as a consequence of an optimal target surface density that reduces steric hindrance and favors the specific adsorption of the DNA 12 mer-AuNPs to the complementary portion of the DNA. From the $\Delta\%R_{\text{match}} / \Delta\%R_{\text{mismatch}}$ ratio between the nanoparticle-enhanced SPRI responses (Figure 6 C), an average value of 3.6 (CV = 19.5%) was obtained in the 1 μ M–1 pm concentration range, while a gradual increase in the ratio values is observed in the 500 fm–1 fm range. In particular, the higher average value is calculated for the 1 fm concentration ($\Delta\%R_{\text{match}} / \Delta\%R_{\text{mismatch}} = 7.4$; SD = 1.2; $n = 5$). This increase can be attributed to the higher dissociation constants of the mismatched sequences,^[30] the responses of which drop to the background level under 1 pm concentration; therefore,

with this approach, which allows DNA to be detected in very diluted samples, an increase in the mismatch recognition is obtained in connection with the decreased detection limits.

The DNA concentrations measured by this method are in a range suitable for detecting DNA samples without amplification, which, in combination with microfluidics and miniaturized devices, could lead to the development of efficient tools for rapid, very specific and direct detection of DNA.

Experimental Section

The PNA oligomer (PNA 1: H-LL-AAACCCTTAATCCCA-NH₂, L: 2-(2-aminoethoxy)ethoxyacetyl spacer, $T_m=64.6^\circ\text{C}$) was synthesized as described elsewhere^[3] (HPLC-MS characterization is reported in the Supporting Information). The sequences of the oligonucleotides (Thermo Fisher Scientific, Inc.) and their acronyms used in this work are shown in Figure 2. All hybridization experiments were carried out in phosphate-buffered saline (PBS, 10 mM) solutions at pH 7.4, with NaCl (137 mM), KCl (2.7 mM) at 25 °C. The SPRI apparatus (GWC Technologies, USA) was the same as reported elsewhere.^[31] Details about the microfluidic devices fabrication and AuNPs synthesis and functionalization are reported as Supporting Information.

Acknowledgements

We thank the MIUR (PRIN 2005 n 2005038704) and the MIPAAF (RIOM project) for financial support. S. Pannitteri is thanked for assistance in TEM measurements.

Keywords: biosensors • DNA • nanostructures • peptide nucleic acids • surface plasmon resonance

- [1] A. Sassolas, B. D. Leca-Bouvier, L. J. Blum, *Chem. Rev.* **2008**, *108*, 109–139.
- [2] J. Xu, S. Zhu, H. Miao, W. Huang, M. Qiu, Y. Huang, X. Fu, Y. Li, *J. Agric. Food Chem.* **2007**, *55*, 5575–5579.
- [3] A. Germini, S. Rossi, A. Zanetti, R. Corradini, C. Fogher, R. Marchelli, *J. Agric. Food Chem.* **2005**, *53*, 3958–3962.
- [4] J. D. Hoheisel, *Nat. Rev. Genet.* **2006**, *7*, 200–210.

- [5] B. Rothenhäusler, W. Knoll, *Nature* **1988**, *332*, 615.
- [6] L. K. Wolf, Y. Gao, R. M. Georgiadis, *J. Am. Chem. Soc.* **2007**, *129*, 10503–10511.
- [7] H. J. Lee, A. W. Wark, R. M. Corn, *Langmuir* **2006**, *22*, 5241–5250.
- [8] R. D'Agata, G. Grasso, G. Iacono, G. Spoto, G. Vecchio, *Org. Biomol. Chem.* **2006**, *4*, 610–612.
- [9] H. J. Lee, T. T. Goodrich, R. M. Corn, *Anal. Chem.* **2001**, *73*, 5525–5531.
- [10] Z. Wang, T. Wilkop, D. Xu, Y. Dong, G. Ma, Q. Cheng, *Anal. Bioanal. Chem.* **2007**, *389*, 819–825.
- [11] L. He, M. D. Musick, S. R. Nicewarner, F. G. Salinas, S. J. Benkovic, M. J. Natan, C. D. Keating, *J. Am. Chem. Soc.* **2000**, *122*, 9071–9077.
- [12] S. Kubitschko, J. Spinke, T. Bruckner, S. Pohl, N. Orantr, *Anal. Biochem.* **1997**, *253*, 112–122.
- [13] T. A. Taton, C. A. Mirkin, R. L. Letsinger, *Science* **2000**, *289*, 1757–1760.
- [14] S. Fang, H. J. Lee, A. W. Wark, R. M. Corn, *J. Am. Chem. Soc.* **2006**, *128*, 14044–14046.
- [15] X. Yao, X. Li, F. Toledo, C. Zurita-Lopez, M. Gutova, J. Momand, F. Zhou, *Anal. Biochem.* **2006**, *354*, 220–228.
- [16] A. Russom, S. Haasl, A. J. Brookes, H. Andersson, G. Stemme, *Anal. Chem.* **2006**, *78*, 2220–2225.
- [17] Y. J. Hu, Z. F. Li, A. M. Diamond, *Anal. Biochem.* **2007**, *369*, 54–59.
- [18] Y. Li, A. W. Wark, H. J. Lee, R. M. Corn, *Anal. Chem.* **2006**, *78*, 3158–3164.
- [19] P. E. Nielsen, *Acc. Chem. Res.* **1999**, *32*, 624–630.
- [20] S. Rossi, E. Scaravelli, A. Germini, R. Corradini, C. Fogher, R. Marchelli, *Eur. Food Res. Technol.* **2006**, *223*, 1–6.
- [21] P. Nielsen, *Q. Rev. Biophys.* **2005**, *38*, 345–350.
- [22] Z. Gao, A. Agarwal, A. D. Trigg, N. F. Singh, T. Cheng, C. H. F. Yi, D. K. Buddharaju, J. Kong, *Anal. Chem.* **2007**, *79*, 3291–3297.
- [23] L.-Q. Chu, R. Foerch, W. Knoll, *Angew. Chem.* **2007**, *119*, 5032–5035; *Angew. Chem. Int. Ed.* **2007**, *46*, 4944–4947.
- [24] R. Gambari, *Curr. Pharm. Des.* **2001**, *7*, 1839–1862.
- [25] J. Liu, L. Tiefenauer, S. Tian, P. E. Nielsen, W. Knoll, *Anal. Chem.* **2006**, *78*, 470–476.
- [26] G. Feriotti, G. Breveglieri, A. Finotti, S. Gardenghi, R. Gambari, *Lab. Invest.* **2004**, *84*, 796–803.
- [27] W. Knoll, H. Park, E. K. Sinner, D. Yao, F. Yu, *Surf. Sci.* **2004**, *570*, 30–42.
- [28] J. Liu, S. Tian, L. Tiefenauer, P. E. Nielsen, W. Knoll, *Anal. Chem.* **2005**, *77*, 2756–2761.
- [29] A. W. Wark, H. J. Lee, A. J. Qavi, R. M. Corn, *Anal. Chem.* **2007**, *79*, 6697–6701.
- [30] T. Ratilainen, A. Holmén, E. Tuite, P. E. Nielsen, B. Nordén, *Biochemistry* **2000**, *39*, 7781–7791.
- [31] G. Grasso, M. Fragai, E. Rizzarelli, G. Spoto, K. J. Yeo, *J. Mass Spectrom.* **2006**, *41*, 1561–1569.

Received: May 6, 2008

Published online on August 4, 2008